PHYSICAL REVIEW VOLUME 184, NUMBER 1 5 AUGUST 1969

Transmission of Coherent Optical Pulses in Gaseous SF_6 †

C. K. Rhodes and A. Szöke
Physics Department, Massachusetts Institute of Technology, Cambridge, Massachusetts 02139
(Received 27 March 1969)

Strong and short coherent pulses of electromagnetic radiation propagate through extended absorbing media with anomalously low absorption, they are delayed and reshaped. This article presents experimental results and calculations for propagation of 10.6-μ wavelength pulses through gaseous SF_6. The degeneracy of overlapping levels of SF_6 in that spectral region is important, and enables us to use a simple model to describe observed phenomena. We assume a continuous distribution of dipole moments. Results are particularly interesting in two regimes of excitation. One corresponds to very strong excitation and ~20 absorption lengths in the medium: Pulses sharpen at their leading edge, while their front part gets absorbed. The other pertains to much lower excitation and only 2 absorption lengths: Reradiation can be distinguished and long delays result which qualitatively resemble the behavior of a two-level system in self-induced transparency. Fairly conclusive agreement is obtained between a previous theoretical treatment of a homogeneously broadened multilevel medium and experiment. The agreement is substantiated by computer calculations. In three Appendixes we present the observation of focusing effects, the theory of an experiment related to transient nutation, and some remarks on photon-echo polarization experiments in optically thick media.

I. INTRODUCTION

A number of results, both experimental and theoretical, have been obtained on the behavior of optical pulse propagation through an absorbing medium. The experiment involved a Q-switched CO_2 laser as the source; the absorbing medium was gaseous SF_6. We also present some experimental results on the spectroscopy of SF_6 which bear on the pulse transmission experiments. On the theoretical side, we present some analytical results based upon a simplified model discussed previously.[1] That model neglects inhomogeneous broadening; in the degenerate case its use is entirely justified. The calculations are substantiated by some considerably more detailed computer results.[2] Both calculations corroborate the experimental findings.

This article emphasizes the influence of level degeneracy (whether spatial or otherwise) on the propagation of coherent radiation. These considerations arise in a natural way in connection with the problems of self-induced transparency[1,3,4] and photon echo.[5,6] It should be pointed out that our experimental findings and interpretation do not agree with some of the results published by Patel and Slusher[4,6] who apparently did not take into account the importance of level degeneracy and the overlap of spectral lines.

The article concludes with three Appendixes. The first presents some unusual observations of pulse reshaping in SF_6. The experimental evidence appears to indicate the presence of a focusing effect.[3] The second Appendix gives the results of calculations relevant to an experiment on CO_2, similar to the transient nutation well known in NMR, that would enable the measurement of the dephasing time T_2. This experiment does not involve a propagation effect. The third contains some remarks on the polarization dependence of the photon echo[5,6] and the modifications that arise for an optically thick sample.

II. EXPERIMENTAL APPARATUS

A schematic of the experimental apparatus is illustrated in Fig. 1. The cavity of the CO_2 laser is bounded by the grating G and the curved Ge mirror M. Q switching is accomplished by the rotating mirror R. Adjustment of the grating G enabled operation on a single vibrational-rotational transition in the 10.6-μ band. The wavelengths were determined by direct measurement with the monochromator K, previously calibrated with a 6328-Å He-Ne laser and corrected to the vacuum. The identification of the particular transitions used in this experiment was unambiguous. A typical output pulse is shown in Fig. 2. Its width is given by $\tau \cong 300$ nsec. The temporal coherence of the pulses was determined by direct examination of the signal modulation generated by beating the Q-switched pulse against an independent continuous wave CO_2 laser in a Au: Ge detector. Since the two lasers were operating independently, the variation of the beat note frequency during the Q-switched pulse establishes an

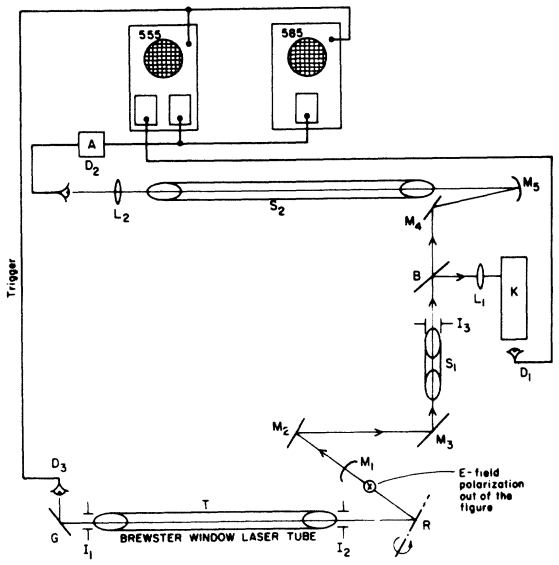

FIG. 1. Schematic diagram of the experimental apparatus. Key: A is the wideband amplifier, rise time ~3 nsec; B is the NaCl flat beam splitter, uncoated; D_1, D_3 are the Ge:Au liquid–N_2 cooled detectors; D_2 is the Ge:Cu liquid-He cooled detector; G is the grating; I_1, I_2, I_3 are the adjustable irises; K is the grating monochromator; L_1, L_2 are the BaF_2 lenses; M_1 is the $7\frac{1}{2}$-m radius Ge mirror, uncoated; M_5 is the 8-m mirror; S_1 is the attenuator cell, 15 cm long; S_2 is the 3.4-m SF_6 absorption cell; R is the flat rotating Q-switch mirror; T is the 3-m Brewster window laser tube.

upper bound on the change of the optical carrier frequency which occurs during the Q-switching process. If $\Delta\omega$ represents the total change in optical frequency during the Q-switched pulse, it was found that $\Delta\omega \lesssim 2\pi/\tau$; hence, enabling one to validly represent the pulse in the form $E(t) = \mathcal{E}(t)\cos\omega t$, with slowly varying $\mathcal{E}(t)$. The pulse intensity was varied by an adjustable linear attenuator. This was accomplished by filling cell S_1 with an appropriate amount of methyl ether (pressure = 1–100 Torr). The linearity of this attenuator is assured by operating at a pressure sufficiently high so that all relaxation rates are $\gg 1/\tau$. A fraction of the input pulse was passed through the monochromator K and detected at detector D_1. The remainder was directed through a 3.4-m SF_6 absorption cell in which the SF_6 pressure could be reliably set to any pressure from 1 mTorr to 10 Torr. This SF_6 pressure was measured by a McLeod gauge. The output pulse was detected at D_2, amplified (if necessary), and photographed directly on the CRT of a Tektronix 585 oscilloscope. The detector D_3 sensed the Q-switched signal which was reflected from the grating zero. This pulse established a trigger signal independent of the intensity of the pulse passing through the cell S_2. Two types of pulse measurements were made. One involved the recording of the signal at D_2 for a fixed SF_6 pressure in cell S_2 while the input pulse intensity was changed by varying the methyl ether pressure in cell S_1. The other corresponded to constant input pulse intensity while the SF_6 pressure in cell S_2 was slowly changed.

The CO_2 laser is of standard design with NaCl Brewster windows and a flowing CO_2-N_2-He gas mixture. Detectors D_1 and D_3 were Ge: Au operated at 77°K while detector D_2 was Ge: Cu operating at liquid-helium temperature. The system rise time (detector and electronics) for detector D_2 was less that 8 nsec as determined by direct measurement.[7]

III. EXPERIMENTAL RESULTS

A. SF_6 Spectroscopic Data

A series of experiments was performed with the object of determining the relative absorption and absorption-versus-pressure behavior of various CO_2 laser oscillations in gaseous SF_6. Figure 3 shows the linear absorption data corresponding to the $P(16)$, $P(18)$, and $P(20)$ CO_2 lines for SF_6 pressures under 50 mTorr. These measurements were made with the apparatus illustrated in Fig. 1 but with the rotating mirror R replaced by a stationary one to permit continuous wave operation, and detector D_2 followed by a lock-in amplifier system. Input signal intensity was ~1 mW. Significant attenuation occurs on all three lines with the $P(16)$ line experiencing the greatest absorption. Since the Doppler width at 10.6 μ for SF_6 is 30 MHz, these lines should be essentially inhomogeneously broadened for the SF_6 pressures less than 50 mTorr. It should be noted that previous work[6] reports observations that are contrary to those shown in Fig. 3. They[6] describe the absorption as appreciable on only one line for SF_6 pressures below 1 Torr and identify this as the $P(20)$ line of CO_2.

The behavior of coherent excitations is strongly

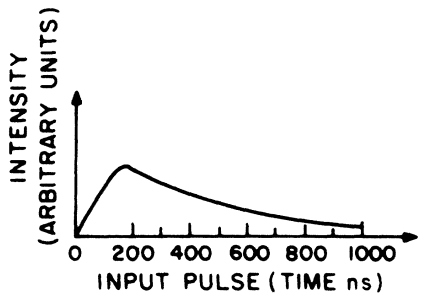

FIG. 2. Typical Q-switched laser pulse. Horizontal scale = 100 nsec/cm.

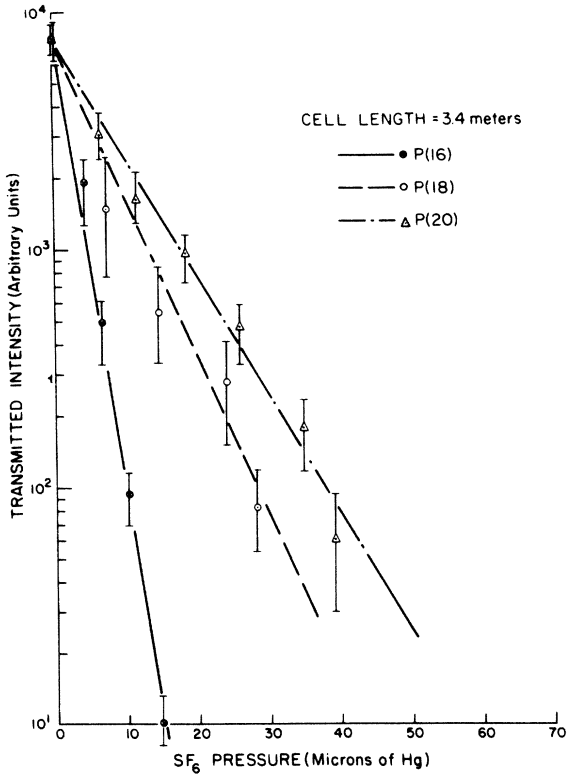

FIG. 3. Linear absorption data for the absorption of the $P(16)$, $P(18)$, and $P(20)$ lines ($10^00 \rightleftharpoons 00^01$ band) of CO_2 in SF_6 for SF_6 pressures below 50 mTorr.

influenced by the precise nature of the states involved. As an example, a simple model describing the effect of spatial degeneracy has previously been described.[1] In the case of SF_6, it is not obvious *a priori* that the transitions in the 10.6-μ band are resolved with respect to their Doppler widths. Indeed, in the region of a Q branch, there is considerable likelihood that this is not the case. For definiteness, let us consider the absorption of the $P(16)$ line of CO_2. If this were caused by a single well-resolved transition, then one would expect the absorption to initially increase linearly with pressure and then become, at sufficiently high pressure, pressure-independent when the transition is fully pressure broadened. At even higher pressure, neighboring lines overlap and the absorption rises again. Experimentally, no such pressure-independent region is observed. On the contrary, the absorption exhibits no inflection points and rises linearly all the way from 0 to 17 Torr, which is well above any reasonable limit for pressure broadening. We believe that this constitutes unequivocal evidence against the hypothesis which states that the strong absorption of $P(16)$ is due to a single well-resolved resonance in SF_6. (See note added in proof.) Similar behavior was also recorded for the $P(18)$-CO_2 line. This is an unfortunate complication, but a crucial one in the understanding of self-induced transparency and photon echo experiments in SF_6.

From a spectroscopic point of view, our findings can be summarized as follows: The $P(16)$ line of CO_2 exhibits the maximum absorption in SF_6, although the $P(18)$ and $P(20)$ lines are also appreciably absorbed. The transitions involved in these absorptions of $P(16)$ and $P(18)$ are not well resolved in relation to their Doppler widths. Figure 4, taken from Brunet,[8] shows the 10.6-μ band of SF_6 and the relative positions of the CO_2 lines according to McCubbin.[9] It is significant that the absorption of the laser radiation is in rough agreement with the low-resolution spectrum obtained by Brunet.[8] This strongly suggests that the band has many overlapping transitions and behaves like a continuum absorber. Indeed, in a later section, a continuum model will be introduced in the description of the behavior of SF_6.

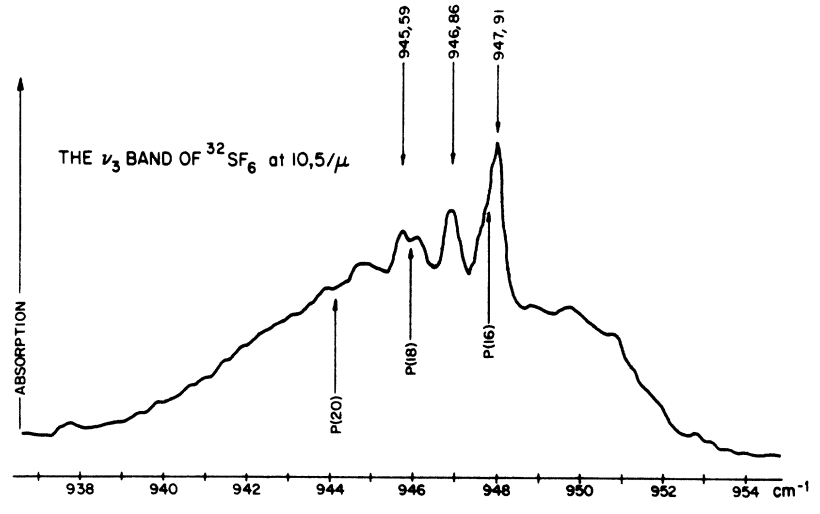

FIG. 4. The SF_6 spectrum in the region of 10.6 μ as taken from Brunet (Ref. 8). The upper numbers are associated wit with points on the SF_6 spectrum. The relative positions of the $P(16)$, $P(18)$, and $P(20)$ transitions of CO_2 are described by the lower arrows.

B. Pulse Experiments Conducted at Low-Radiation Intensity and Low SF_6 Pressure (~10 mTorr)

In order to examine carefully the transition from the linear absorption region to the nonlinear region, we worked at greatly reduced intensities for these runs ($\sim 10^{-3}$ of available intensity). We also operated at low pressures (~10-mTorr SF_6) so that the inequality $T_2 \gg \tau = 300$ nsec would be beyond suspicion. In particular, we were concerned with the time delay of pulses in this nonlinear transition region together with the relative intensities of the transmitted radiation. It should be pointed out that the electronics were all triggered by detector D_3 which was independent of the intensities of the incident and transmitted pulses. Thus, the relative positions of the photographed pulses with respect to one another are real, not artificial. Three CO_2 transitions were examined in detail: $P(16)$, $P(18)$, and $P(20)$. Figure 5 illustrates a sequence of output pulses, at constant SF_6 pressure, for varying input amplitude of the $P(16)$ lines. The first pulse in the sequence was nearly the minimum detectable intensity; its shape is that of the input pulse and its delay is observed to be very small. As the input intensity is raised,

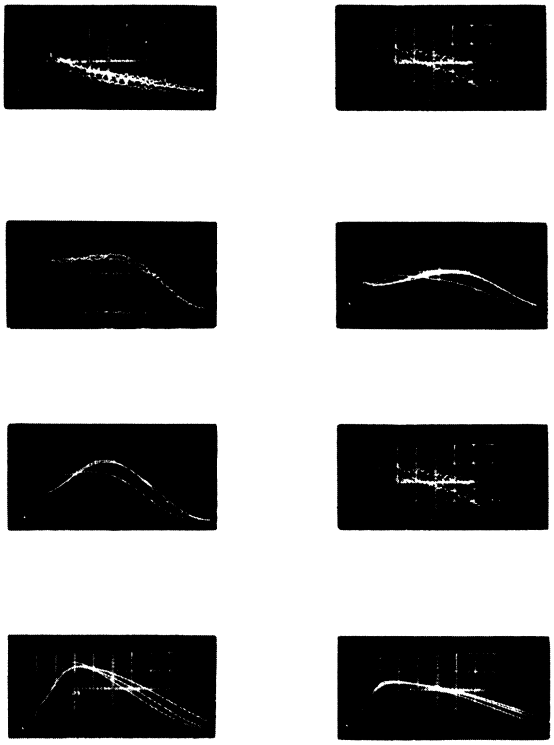

FIG. 5. A sequence of output pulses at an SF_6 pressure of 6 mTorr, for varying input intensity of the CO_2 $P(16)$ transition. In the sequence, the input intensity rises monotonically from the top left to the lower right reading successively across the page. The time scale for all photographs is 100 nsec/cm.

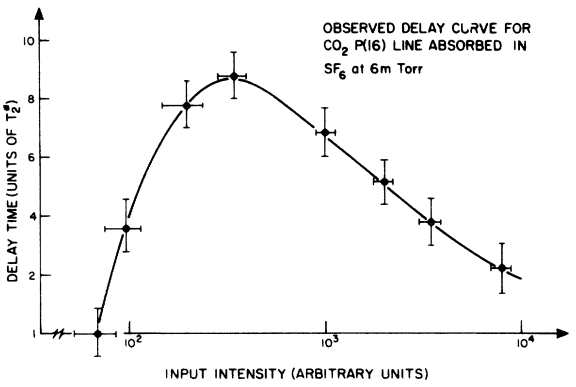

FIG. 6. A delay curve; the position of the output pulse maximum versus the input pulse intensity of the CO_2 $P(16)$ line. The SF_6 pressure was 6 mTorr. The delay times are in units of the SF_6 inhomogeneous width, $T_2^* = 50$ nsec.

the delay is observed to increase while the pulse reshapes dramatically. As the input intensity is raised further, the delay of the pulse peak is reduced, and the pulse assumes the shape corresponding to the input pulse. Figure 6 illustrates the relative time position of the output pulse peak as a function of output intensity for the $P(16)$ transition. It is significant to note that the reversal of the delay curve, Fig. 6, occurs at an intensity which corresponds to the knee (inflection point) of the saturation curve, Fig. 7. Some recent calculations by Hopf and Scully[10] indicate such effects. Similar behavior was noted on both the $P(18)$ and $P(20)$ transitions. However, in these cases, the results are not as prominent, since the $P(18)$ and $P(20)$ lines are absorbed less strongly than the $P(16)$. However, a central point remains; the behaviors of all three transitions $P(16)$, $P(18)$, and $P(20)$ were qualitatively similar.

The sequence of photographs in Fig. 5 shows that the pulses possess a sharp peak at the leading edge corresponding to the sharp peak at the front of the input pulse. This small peak has precursor-type behavior. The saturation curve for this peak drawn in Fig. 7 shows that it is transmitted linearly as a function of input intensity in contrast to the remainder of the pulse.

C. Pulse Experiments Conducted at High-Radiation Intensity and Moderate SF_6 Pressure (~40 mTorr)

An interesting effect was observed at high input intensities, i.e., intensities well above the knee on the saturation curve shown in Fig. 7. In this experiment, the input intensity was held constant while the pressure in the SF_6 cell was continuously lowered at a slow pumping rate. Figure 8 shows a sequence of photographs taken during one

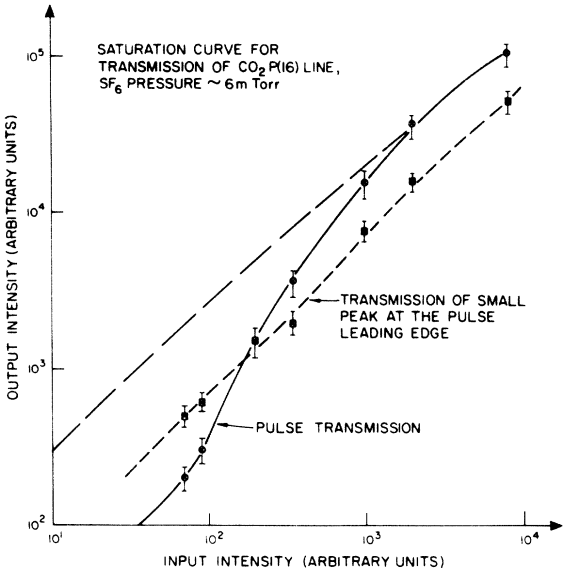

FIG. 7. The saturation curve which corresponds to the data illustrated in Fig. 6; output pulse intensity versus input pulse intensity. The SF_6 pressure was 6 mTorr. The small peak on the input pulse has precursor-type behavior as indicated by the linear plot that represents its response.

such run for the $P(16)$ transition of CO_2. The largest pulse corresponds to an empty cell and thus, is really the input pulse itself. The other pulses are at progressively higher pressure, in the obvious order. The photograph clearly shows a reshaping of the leading edge at an intermediate SF_6 pressure around 40 ~ 50 mTorr. This steepening corresponds to a rise time of 30 nsec. Care

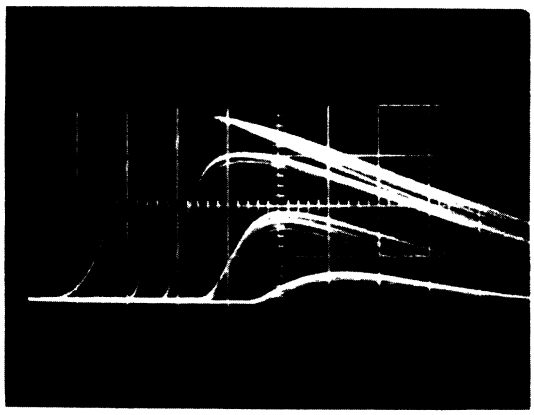

FIG. 8. An output pulse sequence for the CO_2 $P(16)$ line as the SF_6 pressure is slowly swept. The pulse steepening occurs at an SF_6 pressure corresponding approximately to 40 mTorr. Pulse intensity is plotted vertically while the time scale on the horizontal is 50 nsec/cm.

must be taken to have a properly loaded detector as ringing can occur which will distort the pulse shape. This steepening can occur from a trival population saturation effect, but as we will show, the behavior also occurs in a system with many overlapping levels even with a fully coherent excitation. This will be called an effective population saturation effect and as in the simple incoherent population saturation effect if corresponds to an energy loss from the propagating pulse. Machine calculations[2] have been made which exhibit this sharpening effect in the limit of coherent excitation, $T_2 > \tau_{\text{pulse}}$. The computations will be described in a later section of this paper. The effect was seen appreciably only on the $P(16)$ line of CO_2; probably on the $P(18)$ and $P(20)$ lines there were not enough absorption lengths in the sample tube.

IV. THEORY AND CALCULATIONS

A. Calculations Corresponding to the Conditions of Sec. III B

In this section, we present a simple model to account for the results obtained at low SF_6 pressure (~ 6 mTorr) and relatively low excitation (i.e., in the region of the knee of the saturation curve Fig. 7). Since the absorption measurements described in Sec. IIIA strongly suggest that a number of overlapping transitions are involved in the absorption of the CO_2 $P(16)$ transition, we introduce a continuous distribution of dipole moments $n(\mu)$. The quantity $n(\mu)\,d\mu$ equals the density of systems possessing dipole moments betwee μ and $\mu + d\mu$. That is, we approximate the true physical situation with an effective continuum of dipole moments. The extent to which this assumption is valid depends upon the nature and density of the overlapping levels. We simply remark that this is not unreasonable, since the Q-branch electric dipole matrix elements for a symmetric top are proportional to the product $mk/j\,(j+1)$ for linearly polarized radiation, where $-j \leq m \leq j$ and $-j \leq k \leq j$, with m and k integral. This dependence, for sufficiently high j, will produce a large distribution of matrix elements, particularly if several overlapping transitions are involved in the absorption.

The basic properties of such a model are illustrated with the choice of $n(\mu) = n_0$ (a constant) for $-\mu_m \leq \mu \leq \mu_m$ and $n(\mu) = 0$ otherwise. As further approximation, it is assumed that all the systems are on exact resonance, $\omega = \omega_0$; any inhomogeneous broadening is ignored and the pulse length τ is regarded as much less than the inverse of the homogeneous linewidth, T_2. These conditions are precisely those presumed in Ref. 1. We define

$$\theta(\mu) \equiv \frac{\mu}{\hbar}\int_{-\infty}^{\infty} \mathcal{E}(t)\,dt \equiv \mu\phi\ , \qquad (1)$$

where $\mathcal{E}(t)$ is the optical electric field amplitude and τ is the pulse width ($\ll$ dephasing time T_2). Then, in analogy with Ref. 1, the polarization density $P(\phi)$ of the medium after the pulse has passed[11] is given by

$$P(\phi) = N \sum_{\{\mu\}} \mu \sin\theta(\mu) - \int_{-\mu_m}^{\mu_m} n(\mu)\mu \sin\theta(\mu) d\mu , \quad (2)$$

where N describes the density of systems, and the sum is converted to an integral because the distribution $n(\mu)$ is continuous (cf. Ref. 1, formulas 5, 7, and 8). The evaluation of the integral in expression (2) yields

$$P(\phi) = 2n_0 \mu_m^{\,2} j_1(\mu_m \phi), \quad (3)$$

where $j_1(x)$ is the spherical Bessel function of the first kind of order one. For comparison, the polarization density $P_1(\phi)$ for a simple nondegenerate two-level system with matrix element μ_0 is written

$$P_1(\phi) = N\mu_0 \sin(\mu_0 \phi) , \quad (4)$$

where N designates the density of atomic systems. Figure 9 shows plots of $|P(\phi)|^2$ and $|P_1(\phi)|^2$ versus ϕ with μ_m/μ_0 appropriately adjusted so that the first zeros of $P(\phi)$ and $P_1(\phi)$ coincide for finite $\phi > 0$. The extent to which the continuum model can be approximated by a two-level system, parametrized with μ_0, in the domain $0 \leq \phi \leq 4.48$ is indicated by the similarity of the two curves. In this region, effects will occur that have a qualitative similarity to self-induced transparency.[3] Considerably greater deviations begin to appear for larger ϕ as a consequence of the coherent dephasing of the ensemble of dipoles. Indeed, in the limit of high excitation the polarization is arbitrarily small since

$$\lim_{\phi \to \infty} P(\phi) = 0.$$

This statement is not true for the nondegenerate system and it constitutes an essential distinction between degenerate and nondegenerate media. A direct implication of this result is that for high excitations (cf. Fig. 9) degenerate systems tend to reradiate very little as compared to the comparable nondegenerate case. Finally, we point out that energy loss is associated with this behavior. Again, following Ref. 1, we calculate the energy loss per unit volume $W(\phi)$ as

$$W(\phi) = \tfrac{1}{2} N\hbar\omega \int n(\mu)[1 - \cos(\phi\mu)] d\mu / \int n(\mu) d\mu \quad (5)$$

giving $$W(\phi) = \tfrac{1}{2} N\hbar\omega [1 - (\sin\phi\mu_m)/\phi\mu_m] . \quad (6)$$

Hence, at high excitations one approaches a constant loss given by

$$\lim_{\phi \to \infty} W(\phi) = \tfrac{1}{2} N\hbar\omega . \quad (7)$$

The loss, coupled with the fact that the degenerate system is qualitatively similar to the nondegenerate case only in the relatively low-excitation range (cf. Fig. 9), restricts the sample thickness for observation of reradiation effects. A sample that is too thin will not absorb and, hence, not reemit. On the other hand, an overly thick sample will present an overwhelming amount of loss, hence, leading to a diminished effect. The maximum observable effect will correspond to an intermediate sample thickness. On this basis the model predicts that coherent reradiation (pulse reshaping) should occur most dramatically at low

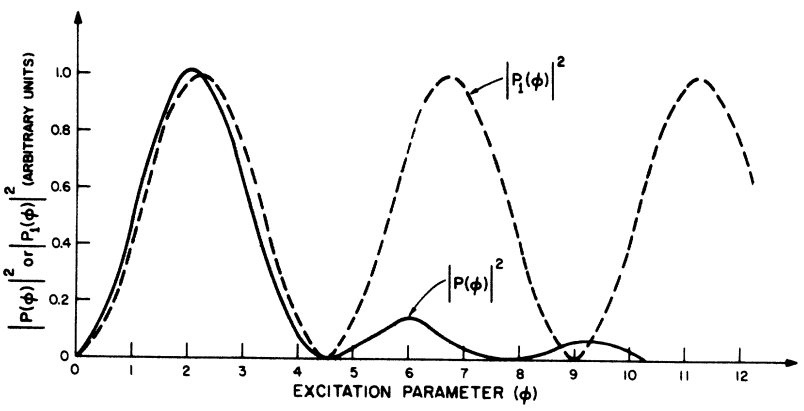

FIG. 9. Plots of the polarization density functions squared, $|P(\phi)|^2$ and $|P_1(\phi)|^2$, for the continuum model and the quasiequivalent two-level system, respectively, versus ϕ The condition for the coincidence of the first zeros of $P(\phi)$ and $P_1(\phi)$ for finite $\phi > 0$ is $\mu_m/\mu_0 = 1.43$.

pressure ($\tau \ll T_2$) and in a narrow range of input intensity for a sample corresponding to a few absorption lengths.[12] Our attitude is supported by both pulse propagation experiments in SF_6 and more detailed computer calculations[2] discussed below.

The experimental behavior, as described in Sec. III B of this article, is substantially in agreement with this simple interpretation. The sample corresponded to nearly two absorption lengths. Examination of Figs. 5 – 7 shows that a significant coherent reradiation effect[13] was observed mainly in the region corresponding to the nonlinear transition region of the saturation curve in Fig. 7. Very little, if any effect, was observed for input intensities above or below this range.

More elaborate computer calculations[2] produced results essentially in agreement with our experimental findings. Specifically, the delay curves agree to within 50%, and the saturation curves fit to within 15%. These computations incorporated the complications of a finite inhomogeneous width, a finite homogeneous width T_2^{-1}, and consequently, rendered a reasonable simulation of the SF_6 experiment. The continuous dipole moment distribution $n(\mu)$, discussed above, was approximated by a uniform distribution of discrete values spaced at equal intervals in μ. Equivalently, the calculations thus performed corresponded to a $Q(10)$ transition of a symmetric top with the k degeneracy removed. The saturation curve, the dependence of the pulse delay on input power, and the broadening of the pulse by reradiation are all very similar to our experimental results. This pulse broadening effect, as in the experiment, disappeared for input conditions corresponding to points either above or below the nonlinear transition region on the saturation curve. It should be noted that the critical input condition for a nondegenerate two-level system would be $\theta_{\text{in}} = \pi$. The computer result for $Q(10)$ indicated a critical situation for $\theta_{\text{in}} \cong 1.4\pi$.[14] Recall that for low exciations we argued that the continuum model could be approximated by a nondegenerate system with an appropriately chosen μ_0(cf. Fig. 9). A value of $\mu_m/\mu_0 = 1.43$ was calculated in that example. We believe that this compares favorably with the factor of 1.4 suggested by the computer results. Of course, such quantitative agreement is completely unexpected in view of the crude estimates that have been made. However, it does inspire respect for the continuum model approximation.

It is worth noting here that in the continuum limit, one can easily estimate the dipole moment distributions corresponding to P-, Q-, or R-branch transitions of a symmetric top. We treat separately the cases distinguished by the presence or absence of k degeneracy and include the effect of inhomogeneous broadening. The quantity $n(\mu, \omega)$ is defined as a density in $\mu - \omega$ space such that $n(\mu, \omega)d\mu\, d\omega$ equals the number of radiators possessing dipole moments between μ and $\mu + d\mu$ with resonant frequencies in an interval between ω and $\omega + d\omega$. The distribution in ω is assumed flat. This is a good approximation when the ratio of the saturation width $\Delta\omega_S = \mu\mathcal{E}/\hbar$ to the inhomogeneous width is less than unity. Hence, it is valid to put $n(\mu, \omega) = n(\mu)\rho(\omega) \propto n(\mu)$. Since $\rho(\omega)$ is a constant, we can integrate over a finite width $\Delta\omega$ giving

$$\int_{\Delta\omega} [n(\mu)\rho(\omega)d\mu]d\omega = n(\mu)\rho(\omega)\,\Delta\omega\, d\mu \equiv n'(\mu)d\mu \,. \tag{8}$$

Now, if the width $\Delta\omega$ is identified as the saturation width, then $n'(\mu) = c\mu n(\mu)$ since the saturation width is proportional to the dipole moment μ. The number c denotes an appropriate proportionality constant which does not concern us here. Hence, the inclusion of inhomogeneous broadening simply multiplies the dipole moment distribution $n(\mu)$ by μ. It remains to calculate $n(\mu)$ for the specific cases. This is accomplished by letting the projection quantum numbers m and k in the matrix elements[15] $\mu_j(m, k)$ represent continuous parameters in the interval $[-j, j]$ and assuming that each value of m or k is equally probable. Only transitions associated with light polarized along the z direction are considered. The results for the Q branches are quoted below. The quantity μ_m denotes the maximum dipole moment of the distributions so the results are valid only in the domain $0 \leq \mu \leq \mu_m$.

(a.) Q branch, k degeneracy removed;
$n'(\mu) \propto \mu$.

(b.) Q branch, k degeneracy unbroken;
$n'(\mu) \propto \mu(\mu_m - \mu)$.

Similar results can be obtained for the P and R branches, although they are somewhat tedious. These distributions show a tendency to peak more nearly about the maximum dipole moment μ_m of the distribution than the Q-branch results.

This section is concluded with some remarks on the intensity dependence of the photon echo.[5,6] These considerations will affect the results of photon echo experiments in that they will lead to a substantial reduction in the echo intensity as a function of the input intensities. Ordinarily, for a nondegenerate system and a thin sample, the echo intensity will be periodic in the input intensities. However, in the continuum model, the echo intensity will be strongly damped at high input intensities, since

$$\lim_{\phi \to \infty} P(\phi) = 0 \,.$$

Indeed, results consistent with this picture have

been reported experimentally.[5] In this work,[5] the echo vanished completely and did not reappear at higher input intensities.

Recapitulating, we have introduced a crude but, we believe, descriptive model for some coherent excitation processes in SF_6. We find that for low excitation, the behavior of the degenerate system qualitatively resembles that of the simple nondegenerate two-level system (cf. Fig. 9). The predictions on pulse reshaping and absorption agree well with both our experimental findings and more sophisticated computer calculations.[2] And finally, it is shown that the anomalous intensity dependence of the photon echo in SF_6 can be understood as arising from the effects of degeneracy.

B. Calculations Corresponding to the Conditions of Sec. III C

The considerations described here pertain to the experimental results of Sec. III C. The entire discussion assumes that no relaxation processes are operative. The principal effect reported in Sec. III C was a considerable sharpening of the leading edge of the pulse under conditions of both high input intensity and an extremely thick sample (~20 absorption lengths). Figure 8, which illustrates this effect, shows that the decrease in the rise time is directly attributable to the energy removed from the leading edge of the pulse. The entire pulse, however, experiences a modest absorption of less than 20% of the total energy and the tail of the pulse is transmitted with no discernible effect. This behavior is typical of a saturation process; the ultimate rise time being determined by the time interval necessary, at that intensity, to saturate the medium. Because of the degeneracy of the SF_6 transition, this saturation behavior will occur even in the limit of a completely coherent excitation. We will call this an "effective" saturation process. It arises because the distribution of dipoles associated with the degeneracy cancel one another at high excitation levels and put the system into a state of essentially zero macroscopic polarization. However, a finite and constant energy is absorbed in this process. Hence, in this context, the term "saturation" describes a situation in which an additional increment of excitation does not change the macroscopic state of the medium, either its polarization or energy content. Naturally, the constant absorption, for a fixed sample, is relatively less and less as the input intensity and energy are increased. Indeed, in the continuum model presented in Sec. III, the macroscopic dipole moment left in the medium after the passage of the pulse is given by Eq. (3). This is a damped oscillating function which decreases rapidly as the pulse angle θ is increased. At the same time, the energy loss per unit volume tends to $\frac{1}{2}N\hbar\omega$ as expression (7) indicates. In order to establish the credibility of this reasoning, we present the following argument: Consider only the leading edge of a pulse whose intensity $I(t)$ is rising linearly as given by

$$I(t) \cong I_0 t/T_r, \quad 0 \leq t \leq T_r . \tag{9}$$

The quantity T_r is defined as the pulse rise time. We assume that the medium is saturated by this leading edge so that

$$\frac{\mu_m}{\hbar}\int_0^{T_r} E(t)\,dt = \frac{\mu_m}{\hbar}\int_0^{T_r} \left(\frac{8\pi}{c} I(t)\right)^{1/2} dt = \theta_m \gg 1 \tag{10}$$

is valid for the characteristic value of the dipole moments associated with the transition. Since I_0 and T_r are known from the experiment, one can calculate a rough estimate for the matrix element μ_m appearing in expression (10). With $I_0 \cong 1$ kW/cm^2, $T_r = 30$ nsec, and assuming $\theta_m \cong 20$, a simple computation gives $\mu_m \cong 3\times10^{-19}$ esu. This value is in good agreement[16] with estimates given for the relevant matrix elements in SF_6. The argument, of course, is only approximate, but since no adjustable parameters are at our disposal, the agreement is significant.

The reasoning and conclusions of the preceding paragraph have been fully substantiated by computer calculations.[2] These calculations take into consideration, level degeneracy, inhomogeneous broadening, and propagation effects arising from an optically thick sample. The radiation field is represented as plane, linearly polarized running wave.[17] Specifically, the computations were performed for a Q-branch transition corresponding to an angular momentum quantum number $j = 10$, $Q(10)$. This particular choice was made because the matrix element distribution for $Q(10)$ provides a discrete approximation to a continuous distribution of matrix elements used for discussion in the preceding Sec. IV A. We are motivated in our selection of a compatible case for discussion here. These calculations, with the parameters appropriately adjusted to correspond to the experimental situation, showed a pulse steepening effect remarkably similar to the one observed. This result is not peculiar to a $Q(10)$ transition. The identical computations were performed for a P-branch transition with angular momentum quantum number $j = 21$, $P(21)$. The conclusion was identical. Thus, as suggested in the remarks leading to Eq. (10), it appears that this pulse steepening effect emerges as a general phenomenon associated with the response of

highly degenerate media to very intense, coherent pulses. In principle, the minimum rise time of this sharpening effect is limited by the effective saturation linewidth of the system. This quantity, from expressions (9) and (10) is given approximately by

$$T_r \cong (3\theta_m \hbar/2\mu_m)(c/8\pi I_0)^{1/2} . \quad (11)$$

This time, T_r can be made arbitrarily small by increasing the intensity I_0.

V. DISCUSSIONS AND CONCLUSIONS

Some of the complications of pulse propagation through an absorbing medium which arise from spatial degeneracy and overlapping levels have been examined both experimentally and theoretically. It is found that the effect of self-induced transparency, first described by McCall and Hahn, [3] is modified in an essential way. These modifications tend to reduce certain features associated with the effect. As is now well known, the strict case of self-induced transparency is only possible under very special circumstances. These conditions are described in Ref. 1. Unfortunately, these modifications tend to destroy many of the features of the pure effect, namely, a finite energy loss is associated with the pulse propagation, delay times are reduced, and the phenomenon of pulse breakup is suppressed. One of the most disappointing features of this result is that all these tendencies qualitatively modify the pulse propagation behavior in the same way as the introduction of a finite T_2. This will inevitably complicate the extraction of information relating to collisions when, in future experiments, one operates in a regime where T_2 is comparable to the pulse width.

Our analysis is based on a degenerate homogeneously broadened model. This is done in order to point out the differences between degenerate and nondegenerate systems. Inhomogeneous broadening, which is present in our experiments, apparently modifies both cases similarly.

Any study of this nature using SF_6 involves obvious difficulties. It has been stressed that the detailed behavior of pulse propagation depends crucially on quantum numbers of the absorbing states. However, the precise level structure of SF_6 is both complicated and unknown. In our analysis, we have attempted to utilize the apparently continuous absorption through the introduction of a continuum model (a continuum in ω and μ). This program views the spectral complications in such a way that a simplification obtains. On this basis a number of statements concerning the behavior of coherent optical excitations were made. All these considerations were in the limiting case of $T_2 \to \infty$. Thus, the main thrust of this research has been focused on the examination of degeneracy effects in a continuum limit. Basically, two different effects were observed and described on the basis of the continuum model. The first involved high excitation of a very thick sample. In this case, an effective saturation behavior was observed which led to a sharpening of the leading edge of the input pulse. This is a fully coherent effect and a general feature of degenerate system under a broad range of circumstances. The second effect illustrated pulse reshaping and reradiation phenomena as they occur in degenerate media. It was shown that under suitable conditions (moderate excitation and a sample around one absorption length) the results could be qualitatively understood by an equivalent two-level system. A finite loss is associated with propagation under all these conditions so no strict transparency is observed. *Note added in proof.* Results that directly confirm our spectroscopic conclusions have been obtained recently by F. Shimizu, Bull. Am. Phys. Soc. 14, 619 (1969); R. L. Abrams and A. Dienes, Appl. Phys. Letters 14, 237 (1969); P. Rabinowitz, R. Keller, and J. T. Latourrette (to be published).

ACKNOWLEDGMENTS

We are indebted to Professor A. Javan for his continued support, encouragement, and advice through the entire course of this work. We also gratefully acknowledge Dr. F. A. Hopf and Professor M. O. Scully for assistance and collaboration on the computer analysis. We cordially express our thanks to P. Hoff and Professor H. Haus for the loan of the detector used in this experiment.

APPENDIX A: UNUSUAL EXPERIMENTAL OBSERVATION IN SF_6

An unusual experimental result was obtained in a pressure and intensity region well above that described in Sec. III B. This result is highly suggestive of a self-focusing effect. The SF_6 pressure in the 3.4-m cell was around 50 mTorr, and the input intensities were approximately 10^3 times above the intensity for maximum pulse reshaping as discussed in Sec. III B. Figure 10 illustrates one such result. The input pulse is essentially the same as shown in Fig. 2. The pulse appears to have broken up into two well-resolved pulses with a node very nearly occurring between them. This pulse configuration, the sharper one traveling faster and both of nearly similar areas, is precisely the waveform to which a 4π input pulse is expected to evolve for a nondegenerate system as discussed by McCall and Hahn. [3] However, this is not happening here, at the very least, in view of the effects of degeneracy. Indeed, careful exami-

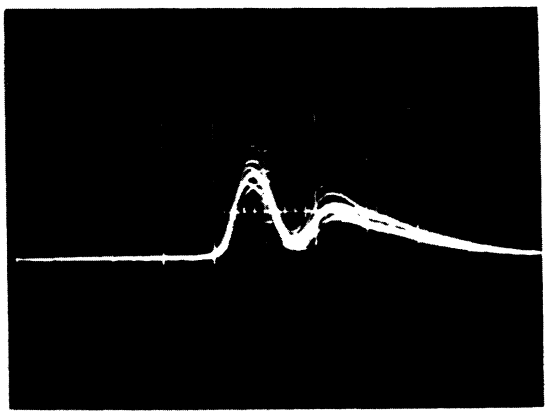

FIG. 10. A double peaked output pulse waveform from the 3.4-m absorption cell. The SF_6 pressure was ~50 mTorr and the input pulse corresponded to that illustrated in Fig. 2. Pulse intensity is plotted vertically while the horizontal time scale corresponds to 50 nsec/cm.

nation indicates that the two peaks are not passing through the same volumes in the absorption cell. The intensity ratio can be reversed by manipulating irises. A complicated phenomenon appears to be taking place. Experimentally, the situation is ripe for violations of an infinite plane-wave description. The sample has an optical depth more than 20 absorption lengths, and our input mode pattern is essentially diffraction limited. The plane-wave model[17] is very probably useless for such circumstances. (i.e., diffracting input and sample absorption lengths $\gg 1$). These effects may be associated with an intensity-dependent delay arising from a nonuniform input beam intensity profile.

APPENDIX B: CO_2 FLUORESCENCE CALCULATIONS

It was stated in the preceding sections of this article, that the unknown spectroscopic properties of SF_6 considerably complicated the analysis of coherent pulse transmission experiments. On the other hand, CO_2, even though it possesses the advantage of a known structure, is practically useless in propagation experiments, because its absorption is too small. In this appendix, we present the results of calculations pertaining to CO_2 in an experimental situation where the known spectroscopic information is used to advantage. It is a variant of the transient nutation effect well known in NMR. The experiment is sensitive to any irreversible dephasing time T_2, but does not operate on a propagation effect. This provides a generous simplification in that only Schrödinger's equation is used in this treatment, Maxwell's equation being unnecessary since no propagation effects are considered (i.e., optically thin medium). CO_2 gas absorbs weakly at 10.6 μ, because the absorption occurs from an excited state ~1300 cm^{-1} above the ground state (see Fig. 11). However, the 4.3-μ transition $00^0 \rightleftharpoons 00^0$ is infrared active and the spontaneous radiation radiated subsequent to excitation at 10.6 μ is readily detectable.[18] For a fully coherent excitation from $10^00 \rightarrow 00^01$ the intensity of the spontaneous emission from the 00^01 state is proportional to the sum of the upper-state populations. We denote the upper-state amplitudes by $a_m(\cdot)$ and consider excitation on only one of the vibrational-rotational transitions in the 10.6-μ band. The spontaneous emission intensity has been calculated as a function of input intensity for a linearly polarized square-wave input pulse of height $\mathcal{E}_0$ and width τ. The effect of inhomogeneous broadening is included. If the upper state amplitudes are assumed to be zero before the pulse, a standard solution of the two-level problem, ignoring antiresonant terms, gives the upper-state populations $|a_m(\Delta\omega, \mathcal{E}_0, \tau)|^2$ as

$$|a_m(\Delta\omega, \mathcal{E}_0, \tau)|^2 = \frac{(\mu_m \mathcal{E}_0)^2}{(\omega-\omega')^2 + (\mu_m \mathcal{E}_0)^2} \times \sin^2\{\tau[(\omega-\omega')^2 + (\mu_m \mathcal{E}_0)]^{1/2}\}, \quad (12)$$

where $\Delta\omega = \omega - \omega'$,

$$\mu_m = \langle \text{upper}, m | \vec{\mu}_{op} | \text{lower}, m \rangle, \quad \hbar = 1,$$

(μ_m is diagonal in m, since input is linearly polarized along the z direction), ω is the angular frequency of optical radiation, and ω' is the angular center frequency of irradiated system.

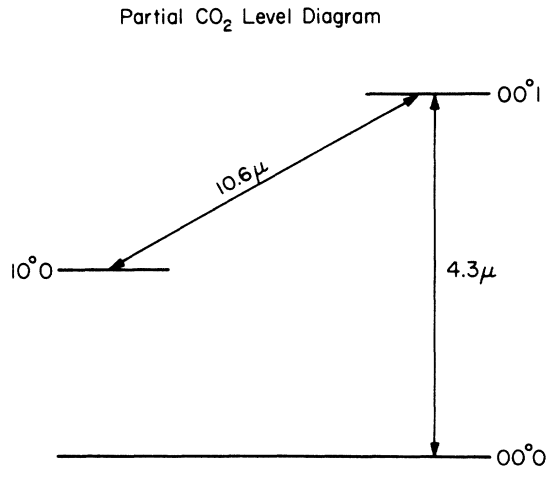

FIG. 11. A partial CO_2 energy level diagram showing the vibrational states relevant to the 10.6-μ absorption and the subsequent 4.3-μ fluorescence.

If the inhomogeneously broadened resonance has a center at ω_0 and is described by a Gaussian distribution of width $\Delta\omega_D$, then the 4.3-μ spontaneous emission signal is proportional to

$$I(\omega, \mathcal{E}_0) = \int_0^\infty d\omega' \exp-\left(\frac{\omega' - \omega_0}{\Delta\omega_D}\right)^2 \sum_{m=-j}^{j} (\mu_m \mathcal{E}_0)^2 \times \frac{\sin^2\{\tau[(\omega-\omega')^2 + (\mu_m \mathcal{E}_0)^2]^{1/2}\}}{(\omega-\omega')^2 + (\mu_m \mathcal{E}_0)^2}. \quad (13)$$

The summation extends over the $2j+1$ degenerate levels associated with the molecular transition. Naturally, we have assumed that $\tau \ll T_2$ in these calculations. We have also ignored any dependence on the input pulse shape as this is known to be weak (square, Gaussian, or hyperbolic secant waveforms probably result in a 5% deviation or less).

Figure 12 illustrates the results for two cases of interest. A curve corresponding to the opposite case $T_2 \ll \tau$, calculated by the normal steady state saturation formula, is included for comparison. The modulation of the output intensity arises from the coherent excitation of states with differing dipole moments.

Experimentally, one measures the 4.3 μ spontaneous emission intensity versus input intensity parametrically as a function of CO_2 pressure. In this way, T_2 can be roughly defined by the pressure at which the intensity modulation becomes smeared. At this pressure $T_2 \sim \tau$. An experiment of this type is presently under way in our laboratory.

APPENDIX C: REMARKS CONCERNING PHOTON ECHO POLARIZATION FOR AN OPTICALLY THICK MEDIUM

Gordon *et al.*[6] have calculated the photon echo polarization dependence on the relative polarization of the excited pulses for P-, Q-, and R-branch transitions for several values of angular momentum j. They give the relative echo polarization under the following conditions: (a) the echo intensity is at a maximum and (b) the sample is optically thin. These results have a dependence on the excitation pulse intensities and will, therefore, not apply to an optically thick medium. Indeed, their experiment, which was conducted on an optically thick sample, led them to conclusions that they themselves described as difficult to believe (to wit $j = 0 \rightleftharpoons j' = 1$ or $j = 1 \rightleftharpoons j' = 1$ transition).

A complete solution of the echo polarization problem involving propagation effects necessitates an elaborate computer analysis which is not presented here. Instead, we indicate how the qualitative effect of a thick sample can be understood in considerably simpler terms as derived from the calculation valid for a thin sample. At this point, we follow the work of Gordon *et al.*[6] in defining a vector $\vec{Q}$ [19] which describes the echo polarization vector by $\epsilon_{\text{echo}} = \vec{Q}/|\vec{Q}|$ and the echo intensity by a quantity proportional to $|\vec{Q}|^2$. Consider the geometry illustrated in Fig. 13. Then $\vec{Q}$ is given[6] by

$$\vec{Q} = \sum_{m,m',m''} \sin\left(\frac{\phi_{2m}}{2}\right) \sin\left(\frac{\phi_{2m'}}{2}\right) \sin(\phi_{1m''}) \times \langle a, m | \vec{P}_{\text{op}} | b, m' \rangle \langle a, m' | e^{-i\psi J_y} | a, m'' \rangle \times \langle b, m'' | e^{i\psi J_y} | b, m \rangle, \quad (14)$$

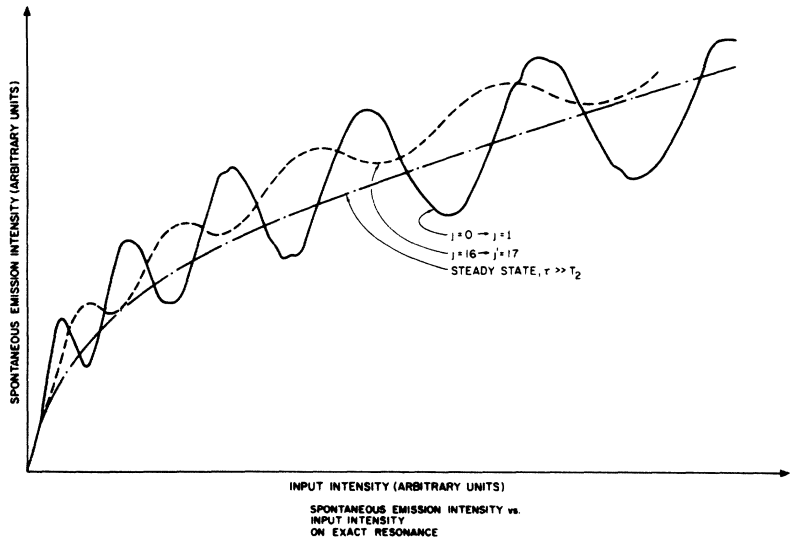

FIG. 12. Intensity of spontaneous emission at 4.3 μ versus intensity ($\mathcal{E}_0^2$) of a square-wave excitation pulse at 10.6 μ. Two cases are shown; $j = 0 \rightarrow j' = 1$ and $j = 16 \rightarrow j' = 17$. The third smooth curve represents the result for a steady state situation, $T_2 \ll \tau$. A Gaussian excitation pulse will produce different curves.

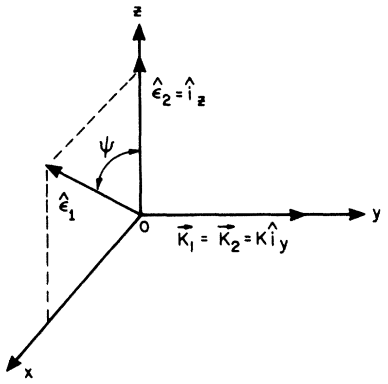

ECHO POLARIZATION GEOMETRY

FIG. 13. The geometry for the echo polarization; $\hat{\epsilon}_1$ is the polarization vector of the first pulse; $\hat{\epsilon}_2 = 1_z$ is the polarization vector of the second pulse; both input pulses propagate along the y axis with wave vector $\vec{k}_1 = \vec{k}_2 = k\hat{i}_y$.

where $\phi_{1i} \equiv 2\langle a,i|P_z|b,i\rangle \int_{\text{first pulse}} F_{1(t)}\,dt$,

$\phi_{2i} \equiv 2\langle b,i|P_z|a,i\rangle \int_{\text{second pulse}} F_{2(t)}\,dt$,

where $F_{i(t)}$ is the envelope of the excitation pulse, $i = 1,2$; $\vec{P}_{op}$ is the dipole moment operator; $\langle a,i|$ is the lower state a,ith sublevel; $\langle b,i|$ is the upper state b,ith sublevel; J_y is the y component of angular momentum operator. The triple summation is taken over all the degenerate sublevels. In a thick sample the excitation functions ϕ_{2i} and ϕ_{1i} vary considerably through the sample. Thus, for $m \neq m'$, the factor $\sin(\phi_{2m}/2)\sin(\phi_{2m'}/2)$, appearing in Eq. (14), will tend to a small quantity due to the effective averaging over a range of ϕ_{2m} and $\phi_{2m'}$. However, for $m = m'$, the $\sin^2(\phi_{2m}/2)$ will tend toward a value of $\frac{1}{2}$. This averaging process then causes the summation to be dominated by the terms for which $m = m'$. The vector property of $\vec{Q}$ is contained in the matrix element $\langle a,m|\vec{P}_{op}|b,m'\rangle$ which for $m = m'$ goes over to $\langle a,m|P_z|b,m\rangle$, P_x and P_y vanishing. Hence $\vec{Q}$ lies along the polarization of the second pulse $\epsilon_2 = 1_z$ independent of the angular momentum quantum states of the participating levels. Of course, this argument is incomplete in that it ignores any propagation effects. In spite of this, however, it fairly clearly establishes the tendency of thick samples with degenerate levels to produce echo polarizations which lie along the second pulse polarization. However, this simple theory does not give a $\cos^2\psi$ dependence for the echo intensity. This intensity behavior is, in general, quite complicated.

---

†Work supported by Air Force Cambridge Research Laboratories and Office of Naval Research.

[1]C. K. Rhodes, A. Szöke, and A. Javan, Phys. Rev. Letters 21, 1151 (1968).

[2]These computer calculations have been performed in collaboration with Dr. F. A. Hopf and Professor M. O Scully. The details of these calculations, along with a number of other results, will appear in a future publication.

[3]S. L. McCall and E L. Hahn, Phys. Rev. Letters 18, 908 (1967).

[4]C. K. N. Patel and R. E. Slusher, Phys. Rev. Letters 19, 1019 (1967).

[5]C. K. N. Patel and R. E. Slusher, Phys. Rev. Letters 20, 1087 (1968); see also, N. A. Kurnit, I.D. Abella, and S. R Hartmann, *ibid.* 13, 567 (1964); and I. D. Abella, N. A. Kurnit, and S. R. Hartmann, Phys. Rev. 141, 391 (1966).

[6]J. P. Gordon, C. H. Wang, C. K. N. Patel, R. E. Slusher, and W. J. Tomlinson, Phys. Rev. 179, 294 (1969).

[7]This result was reported to us by Mr. P. Hoff and Professor H. Haus, from whom the detector was borrowed. Also see T. Bridges, H. Haus, and P. Hoff, Appl. Phys. Letters 13, 316 (1968).

[8]H. Brunet, Compt. Rend. 264, 1721 (1967).

[9]T. K. McCubbin, Jr., U.S. Air Force Cambridge Research Laboratories Report No. AFCRL-67-0437, 1967 (unpublished).

[10]F. A. Hopf and M. O. Scully (to be published).

[11]The "passing" of the input pulse can be distinguished only if $P(\phi)$ is small, otherwise appreciable ringing will occur and the pulse will appear to broaden. This weakness is inherent in any treatment that uses a homogeneously broadened model. Hence, we will regard expressions (2)–(7) as valid for ranges of ϕ, where $P(\phi)$ is sufficiently small. These ranges will occur near the zeros of $P(\phi)$ and for ϕ large, since $|P(\phi)|$ decreases rapidly as ϕ increases (cf. Fig. 9).

[12]We appreciate that this point is not too precise. However, for samples of less than two absorption lengths and for input intensities in the region of the knee of the saturation curve (cf. Fig. 7) the excitation throughout the sample is roughly uniform. We argue further, that in such low absorption samples, the reradiated energy can be considered in a first approximation as essentially unaffected by this absorption (see Ref. 13).

[13]R. H. Dicke, Phys. Rev. 93, 99 (1954); N. Bloembergen and R. V. Pound, *ibid.* 95, 8 (1954); S. Bloom, J. Appl. Phys. 28, 800 (1957).

[14]The angle θ_{in} is calculated with respect to μ_m, which, in this case, is equal to unity.

[15]C. H. Townes and A. L. Schawlow, Microwave Spectroscopy (McGraw-Hill Book Company, Inc., New York,

1955), p. 96.

[16]From low-level absorption experiments, we estimate the value of the average matrix element associated with this absorption as $\sim 5 \times 10^{-19}$ esu. Professor J. Steinfeld, in an independent study, estimates a value of $\sim 3 \times 10^{-19}$ esu (private communication).

[17]It is important to observe that this plane-wave assumption automatically excludes from consideration all phenomena associated with the curvature of surfaces of constant phase. An important example is self-focusing.

[18]L. O. Hocker, M. A. Kovacs, C. K. Rhodes, G. W. Flynn, and A. Javan, Phys. Rev. Letters 17, 233 (1966).

[19]For a derivation of $\vec{Q}$, the interested reader should see Ref. 6. They (Ref. 6) calculate the response of the medium using standard density matrix methods and then isolate the term responsible for the echo. This modulo, a multiplicative factor, is $\vec{Q}$.

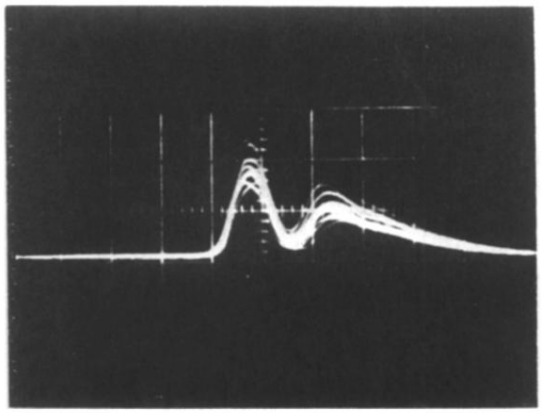

FIG. 10. A double peaked output pulse waveform from the 3.4-m absorption cell. The SF_6 pressure was ~50 mTorr and the input pulse corresponded to that illustrated in Fig. 2. Pulse intensity is plotted vertically while the horizontal time scale corresponds to 50 nsec/cm.

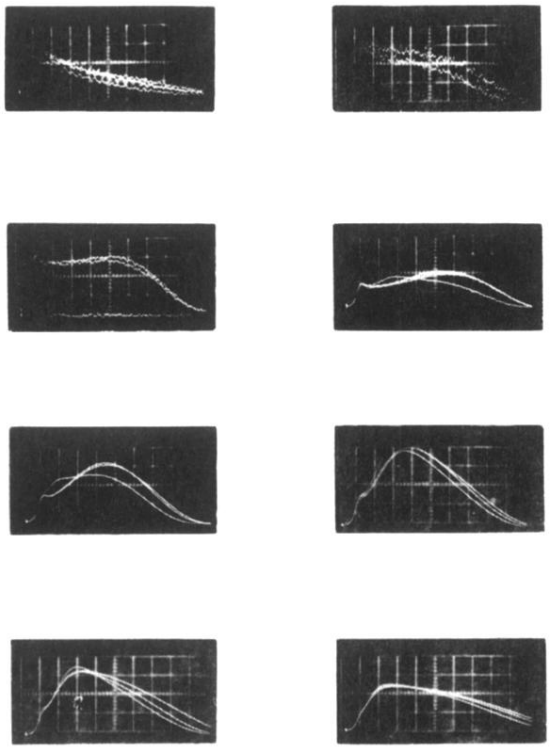

FIG. 5. A sequence of output pulses at an SF_6 pressure of 6 mTorr, for varying input intensity of the CO_2 $P(16)$ transition. In the sequence, the input intensity rises monotonically from the top left to the lower right reading successively across the page. The time scale for all photographs is 100 nsec/cm.

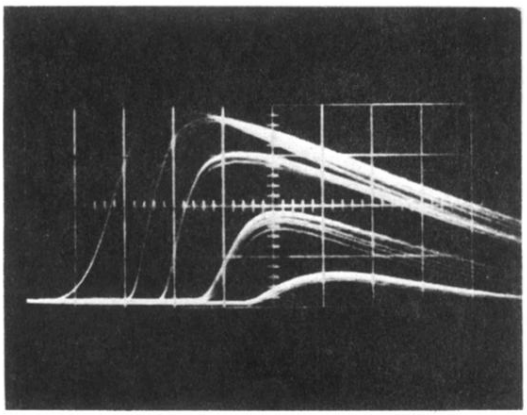

FIG. 8. An output pulse sequence for the CO_2 $P(16)$ line as the SF_6 pressure is slowly swept. The pulse steepening occurs at an SF_6 pressure corresponding approximately to 40 mTorr. Pulse intensity is plotted vertically while the time scale on the horizontal is 50 nsec/cm.